

Numerical Heat Transfer, Part B: Fundamentals



ISSN: 1040-7790 (Print) 1521-0626 (Online) Journal homepage: http://www.tandfonline.com/loi/unhb20

A NEW HIGH-RESOLUTION SCHEME BASED ON THE NORMALIZED VARIABLE FORMULATION

M. S. Darwish

To cite this article: M. S. Darwish (1993) A NEW HIGH-RESOLUTION SCHEME BASED ON THE NORMALIZED VARIABLE FORMULATION, Numerical Heat Transfer, Part B: Fundamentals, 24:3, 353-371, DOI: 10.1080/10407799308955898

To link to this article: http://dx.doi.org/10.1080/10407799308955898

	Published online: 07 May 2007.
	Submit your article to this journal $oldsymbol{G}$
lılı	Article views: 73
Q	View related articles 🗗
4	Citing articles: 64 View citing articles 🗗

Full Terms & Conditions of access and use can be found at http://www.tandfonline.com/action/journalInformation?journalCode=unhb20

A NEW HIGH-RESOLUTION SCHEME BASED ON THE NORMALIZED VARIABLE FORMULATION

M. S. Darwish

American University of Beirut, Faculty of Engineering & Architecture, Mechanical Engineering Department, Beirut, Lebanon

A high-resolution (HR) discretization scheme is proposed for the calculation of incompressible steady-state convective flow with finite-volume methods. The basic algorithm combines a second- and third-order interpolation profile applied in the context of the normalized variable formulation (NVF). The new scheme is tested by solving three problems: (1) a two-dimensional pure convection of a scalar involving a step profile in an oblique velocity field; (2) a two-dimensional pure convection of a scalar involving an elliptic profile in an oblique velocity field; (3) the Smith-Hutton [1] problem involving pure convection of a step profile in a rotational velocity field. The computational results obtained are compared with the results of six HR schemes: Leonard's EULER scheme, Gaskell and Lau's SMART scheme, Van Leer's CLAM and MUSCL schemes, Chakravarthy and Osher's OSHER scheme, Roe's MINMOD scheme, and the exact solution. The results for the new scheme, STOIC demonstrate its capability in capturing steep gradients while maintaining the boundedness of solutions. Furthermore, the comparison with other HR schemes shows that the STOIC scheme yields the most accurate results without undue physical oscillations or numerical smearing.

INTRODUCTION

The accurate simulation of convection continues to attract a large number of workers due to the many challenges it still offers. The difficulty in devising a high-accuracy bounded scheme lies in the conflicting requirements of accuracy on one hand, and stability and boundedness on the other. While stability and boundedness require some kind of diffusive smoothing mechanism, accuracy relies precisely on the opposite. In recent years, a variety of so-called higher-order schemes have been presented, such as the QUICK scheme of Leonard [2], the third-order scheme of Agarwal [3], and the second-order upwind scheme of Fromm [4]. These higher-order schemes certainly yield more accurate results than the highly diffusive first-order upwind scheme, and are certainly more stable than the second-order central difference scheme, but it is now well known that they suffer from a lack of boundedness, that is, they tend to give rise to oscillations or under/overshoots, especially in regions of strong gradients, as is mentioned in [5, 6]. These under/overshoots can induce large errors and lead to unphysical results, and in some cases prevent convergence of calculation when nonnegative scalars (e.g., concentrations or turbulent quantities such as k and ϵ) become negative.

NOMENCLATURE					
а	coefficients of the discretized equation	Superscripts	•		
b	source term in the discretized	C	convection contribution		
	equation	D	diffusion contribution		
В	volume integral of Q	U	upwind formulation		
C f()	convective flux coefficient functional relationship	-	refers to normalized variable		
J	total scalar flux across cell face	Subscripts			
Q	source term in the transport				
	equation	C	central grid point		
RE	residual error	D	downstream grid point		
S	surface area of control volume	dc	deferred correction		
	face or source term	e, w, n, s	refers to control volume faces		
u, v	velocity components in the x and y directions	E, W, N, S	refers to neighbors of grid point P		
Γ	diffusion	f	refers to any of the control		
ϵ	quantitative indicator of error		volume face		
ρ	density	nb	refers to neighbors		
φ	general dependent variable	P	main grid point		
		U	upstream grid point		

For the suppression of these oscillations, a variety of procedures have been developed. These procedures can be grouped along two lines. One approach is to follow a blending strategy, where one either adds a limited antidiffusive flux to a first-order upwind scheme in such a way as to ensure that the resulting scheme is capable of resolving sharp gradients without undue under/overshoots; or, on the contrary, one introduces some kind of smoothing diffusive agencies into an unbounded or higher-order scheme to damp oscillations. The flux-corrected transport (FCT) method of Zalesak [7] is an example of the first type of flux-blending technique, while examples of the second type are the filtering remedy and methodology (FRAM) of Chapman [8], and the flux-blending methods of Peric [9] and Zhu and Leschziner [10]. The determination of the blending factor, usually based on the local solution behavior, is critical to the successful application of such methods. Also, because of their multistep nature, flux-blending techniques tend to be very expensive computationally and/or they are often unable to provide the desired "optimum blend" between accuracy and boundedness. Hence, although fluxblending methods are much more accurate than the first-order upwind scheme, these methods still generate an unnecessary degree of numerical diffusion when attempting to simulate sharp gradients. It should be pointed out that the hybrid scheme of Spalding [11], and the power law scheme of Patankar [12], can be classified as flux-blending schemes, where the blending criterion is based on the local Peclet number rather than on the local solution behavior. The simplicity of these schemes is, however, more than offset by the level of overdamping added to the solution.

A better way to remove unphysical oscillation is to use a composite flux limiter approach. In composite high-resolution (HR) schemes, the numerical flux at

the interface of the computational cell is modified by the use of a flux limiter that enforces a monotonicity (boundedness) criterion. The family of "shock-capturing" schemes based on the total variational diminishing flux limiters (TVD) [13], widely used in compressible flow simulations, is a well-known example of composite schemes. A more recent formulation for high-resolution flux limiters has been developed by Leonard based on the normalized variables formulation (NVF) [14], which since its introduction in 1981 [15] has attracted a growing number of workers such as Zhu and Rodi [16], Gaskell and Lau [17], Zhu [18], and Lin and Chieng [19] to cite a few.

In this article a composite high-resolution scheme, based on the NVF methodology, is proposed for approximating the convection terms of steady-state incompressible transport equations within the framework of finite-volume calculations. This scheme will be compared with six other composite schemes. The schemes are Van Leer's MUSCL [20] and CLAM (curved line advection method) [21], Chakravarthy and Osher's OSHER [22], the MINMOD (minimum modulus) of Roe [23], Leonard's EULER [24], and Gaskell and Lau's SMART [17]. (It was found that the SOUCOUP scheme of Zhu and Rodi [16] is similar to the MINMOD scheme of Roe, and the HLPA of Zhu [18] is similar to Van Leer's CLAM scheme.) All the tested schemes are expressed using the normalized variable formulation [14, 25], so after the introduction of the governing equations, the normalized variable is presented along with the convection boundedness criteria (CBC) [17], which forms the monotonicity criterion for NVF-based flux limiters.

NUMERICAL DISCRETIZATION OF THE TRANSPORT EQUATION

The transport equation governing two-dimensional incompressible steady flows may be expressed in the following general form:

$$\frac{\partial}{\partial x} \left(\rho u \phi - \Gamma \frac{\partial \phi}{\partial x} \right) + \frac{\partial}{\partial y} \left(\rho v \phi - \Gamma \frac{\partial \phi}{\partial y} \right) = Q \tag{1}$$

where ϕ is any dependent variable, u and v are the x and y components of the velocity vector, and ρ , Γ , and Q are the density, diffusivity, and source terms, respectively. Integrating the above equation over the control volume shown in Fig. 1 and using the divergence theorem, we get, for a Cartesian coordinate system, the following discretized equation:

$$J_{e} - J_{w} + J_{n} - J_{s} = B \tag{2}$$

where J_f represent the total flux of ϕ across face f (f = e, w, n, or s), and B is the volume integral of the source term Q. Each of the surface fluxes J_f contains a convective contribution, J_f^C , and a diffusive contribution, J_f^D , hence

$$J_{\rm f} = J_{\rm f}^{\rm C} + J_{\rm f}^{\rm D} \tag{3}$$

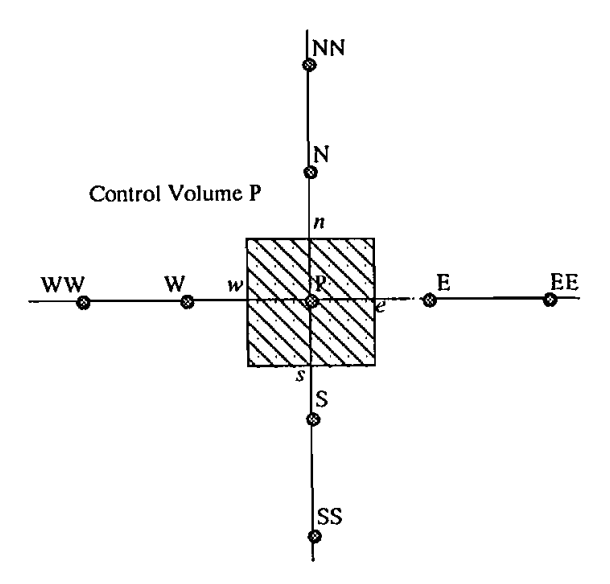


Fig. 1 Typical grid-point cluster and control volume.

For a purely convective scalar flow, the diffusion flux $J_{\rm f}^{\rm D}$ is zero, while the convective flux is given by

$$J_{\rm f}^{\rm C} = (\rho \mathbf{u} \cdot \mathbf{S})_{\rm f} \phi_{\rm f} = C_{\rm f} \phi_{\rm f} \tag{4}$$

where S_f is the surface of cell face f, and C_f is the convective flux coefficient of cell face f. As can be seen from Eq. (4), the accuracy of the control-volume solution for the convective scalar flux depends on the proper estimation of the face value of ϕ_f as a function of the neighboring ϕ node values. Using some assumed interpolation profile, ϕ_f can be formulated explicitly in terms of its neighboring node values by a functional relationship of the form

$$\phi_{\rm f} = f(\phi_{\rm nb}) \tag{5}$$

where ϕ_{nb} denotes the neighboring node ϕ values. After substituting Eq. (5) into Eq. (4) for each cell face, Eq. (2) is transformed after some algebraic manipulations into the following discretization equation:

$$a_{\mathrm{P}}\phi_{\mathrm{P}} = \sum_{\mathrm{nb}} (a_{\mathrm{nb}}\phi_{\mathrm{nb}}) + b_{\mathrm{P}} \tag{6}$$

where the coefficients a_P, a_E, \ldots depend on the selected scheme and b_P is the source term of the discretized equation.

Since the functional derivative can involve a large number of neighboring points, especially when using higher-order schemes, the solution of Eq. (6) can become very expensive computationally, hence the use of a compacting procedure is most welcome. In the present work the deferred correction procedure of Khosla

et al. [26] is used. In this procedure Eq. (2) is rewritten as

$$J_{c}^{U} - J_{w}^{U} + J_{n}^{U} - J_{s}^{U}$$

$$= B + \left[C_{c} (\phi_{e}^{U} - \phi_{e}) - C_{w} (\phi_{w}^{U} - \phi_{w}) + C_{n} (\phi_{n}^{U} - \phi_{n}) - C_{s} (\phi_{s}^{U} - \phi_{s}) \right]$$
(7)

where ϕ_f^U is the face value, J_f^U is the total flux of ϕ , both calculated using the first-order upwind scheme, ϕ_f is the face value calculated using the chosen high-resolution scheme, and the terms in square brackets represent the extra source term due to the deferred correction. Substituting the value of the cell flux obtained from the functional relationship of the upwind and high-resolution scheme at hand, the deferred correction results in an equation similar in form to Eq. (6), but where the coefficient matrix is pentadiagonal (for 2D) and always diagonally dominant, since it is formed using the first-order upwind scheme. The discretized equation, Eq. (6), becomes

$$a_{\rm P}\phi_{\rm P} = \sum_{\rm nb} (a_{\rm nb}\phi_{\rm nb}) + b_{\rm P} + b_{\rm dc}$$
 (8)

where now the coefficients $a_{\rm P}, a_{\rm E}, \ldots$ are obtained from a first-order upwind discretization, nb = (E, W, S, N), and $b_{\rm dc}$ is the extra deferred correction source term. This compacting procedure is simple to implement and effective when using higher-order or high-resolution schemes.

THE NORMALIZED VARIABLE FORMULATION

The Normalized Variable

The proposed scheme is formulated on the basis of the normalized variable proposed by Leonard [12]. Considering face f of a control volume (see Fig. 2a), defining ϕ_U , ϕ_D , ϕ_C , and ϕ_f as the upstream (U), downstream (D), central nodal values (C), and face value (f) for each cell face (see Fig. 2b), the normalized variable is defined as

$$\tilde{\phi} = \frac{\phi - \phi_{\text{U}}}{\phi_{\text{D}} - \phi_{\text{U}}} \tag{9}$$

Note that with this normalization $\tilde{\phi}_D = 1$ and $\tilde{\phi}_U = 0$. The use of the normalized variable simplifies the definition of the functional relationships of HR schemes and will be helpful in defining the conditions that the functional relationships should satisfy in order to have the property of boundedness and stability.

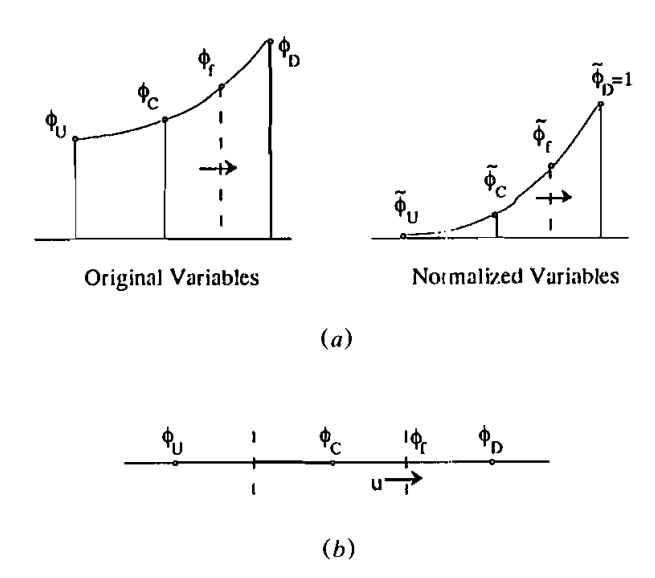


Fig. 2 (a) Original and normalized variables and profiles and (b) the interpolation points used in calculating ϕ_f .

For example, the functional relationship for Van Leer's CLAM scheme for steady flow is given by

$$\phi_{f} = f(\phi_{U}, \phi_{C}, \phi_{D})$$

$$= \begin{cases} \phi_{C} & \text{if } |\phi_{D} - 2\phi_{C} + \phi_{U}| > |\phi_{D} - \phi_{U}| \\ \phi_{C} + \frac{(\phi_{D} - \phi_{C})(\phi_{C} - \phi_{U})}{(\phi_{D} - \phi_{U})} & \text{otherwise} \end{cases}$$

$$(10)$$

Using the normalized variable, Eq. (10) becomes

$$\tilde{\phi}_{f} = f(\tilde{\phi}_{C}) = \begin{cases} \tilde{\phi}_{C} & \text{if } \tilde{\phi}_{C} < 0 \text{ or } \tilde{\phi}_{C} > 1\\ \tilde{\phi}_{C}(2 - \tilde{\phi}_{C}) & \text{otherwise} \end{cases}$$
(11)

A number of schemes written using the normalized variable formulation are given in Table 1, including the QUICK scheme of Leonard [2], the central difference scheme, Fromm's scheme [4], the second-order upwind scheme, and the first-order upwind scheme. Note that the functional relationships for these schemes are all linear functions of $\tilde{\phi}_{\rm C}$.

The functional relationship of any scheme can be plotted in a normalized variable diagram (NVD), that is, by plotting $\tilde{\phi}_f$ versus $\tilde{\phi}_C$. Figure 3 shows the normalized variable diagram for the schemes of Table 1. The NVD can be

Table 1 Functional Relationships for the Different Linear Schemes

Scheme	Functional relationship	Functional relationship (NVF)
First-order upwinding (T.1) Second-order upwinding (T.2)	$\phi_{\mathrm{f}} = \phi_{C}$	$ ilde{\phi}_{\mathrm{f}} = ilde{\phi}_{\mathrm{C}}$
(extrapolation of linear fit through $\phi_{\rm C}$ and $\Phi_{\rm U}$)	$\phi_{\rm f} = \frac{3\phi_{\rm C} - \phi_{\rm U}}{2}$	$ ilde{\phi}_{\mathrm{f}} = rac{3}{2} ilde{\phi}_{\mathrm{C}}$
Lax-Wendroff method (T.3) (interpolation of linear linear fit through $\phi_{\rm C}$ and $\phi_{\rm D}$)	$\phi_{\rm f} = \frac{\phi_D + \phi_C}{2}$	$ ilde{\phi}_{ m f} = rac{1}{2}(1+ ilde{\phi}_{ m C})$
Fromm's method (T.4) [arithmetic mean of (T.2) and (T.3)]	$\phi_{\rm f} = \phi_{\rm C} + \frac{\phi_D - \phi_U}{4}$	$ ilde{\phi}_{\mathrm{f}} = rac{1}{4} + ilde{\phi}_{\mathrm{C}}$
QUICK (T.5) (interpolation of quadratic fit through ϕ_U , ϕ_C , and ϕ_D)	$\phi_{\rm f} = \frac{\phi_{\rm C} + \phi_{\rm D}}{2} - \frac{\phi_{\rm D} - 2\phi_{\rm C} + \phi_{\rm U}}{8}$	$\tilde{\phi}_{\rm f} = \frac{3}{8} + \frac{3}{4}\tilde{\phi}_{\rm C}$

an effective tool in assessing the accuracy and relative diffusivity of schemes. For example, Leonard has shown in [14] that any scheme that has a functional relationship passing through point Q in Fig. 3 is at least second order, and that if the slope at point Q is equal to 0.75, then the scheme is third-order accurate. Also, schemes that have an NVD plot that is near to the first-order upwind NVD plot

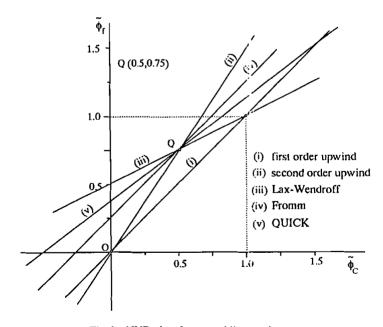


Fig. 3 NVD plots for several linear schemes.

tend to be highly diffusive, while schemes whose NVD plot is near the first-order downwind NVD plot (the line $\tilde{\phi}_f = 1$) tend to be highly compressive.

The Convective Boundedness Criteria (CBC)

Based on the normalized variable analysis, Gaskell and Lau [17] formulated a convection boundedness criterion (CBC) for implicit steady-state flow calculation, which states that for a scheme to have boundedness property, its functional relationship should be continuous, should be bounded from below by $\tilde{\phi}_{\rm f} = \tilde{\phi}_{\rm C}$, and from above by unity, and should pass through the points (0,0) and (1,1), in the monotonic range $(0<\tilde{\phi}_{\rm C}<1)$, and for $1<\tilde{\phi}_{\rm C}$ or $\phi_{\rm C}<0$, the functional relationship $f(\tilde{\phi}_{\rm C})$ should equal $\tilde{\phi}_{\rm C}$.

The above conditions, illustrated in Fig. 4, can be formulated as

$$\begin{cases} f(\tilde{\phi}_{C}) \text{ is continuous} \\ f(\tilde{\phi}_{C}) = 0 & \text{for } \tilde{\phi}_{C} = 0 \\ f(\tilde{\phi}_{C}) = 1 & \text{for } \tilde{\phi}_{C} = 1 \\ f(\tilde{\phi}_{C}) < 1 \text{ and } f(\tilde{\phi}_{C}) > \tilde{\phi}_{C} & \text{for } 0 < \tilde{\phi}_{C} < 1 \\ f(\tilde{\phi}_{C}) = \tilde{\phi}_{C} & \text{for } \tilde{\phi}_{C} < 0 \text{ or } \tilde{\phi}_{C} > 1 \end{cases}$$

$$(12)$$

It is evident from Table 1 and Fig. 3 that none of the five linear schemes can achieve monotonicity and high accuracy simultaneously, the UPWIND scheme being the only linear scheme that satisfies the boundedness criteria. In order to construct a high-resolution bounded scheme, the use of a nonlinear functional relationship is unavoidable.

The STOIC Scheme

The present work assumes that the normalized variable at the cell face, $\tilde{\phi}_{\rm f}$, can be related to the normalized variable at the center, $\tilde{\phi}_{\rm C}$, by a combination of

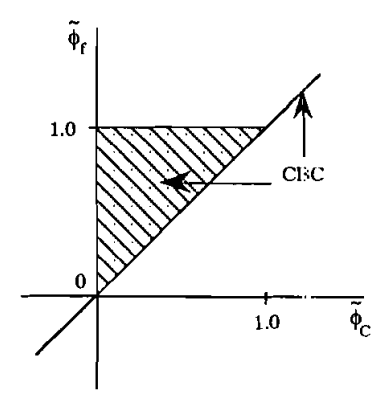


Fig. 4 Convective boundedness criterion (CBC).

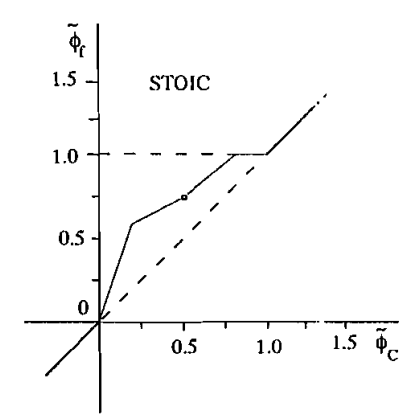


Fig. 5 NVD plots for the STOIC high-resolution schemes

linear functions. In the monotonic range, the second-order central difference scheme and the third-order QUICK scheme are combined in the manner shown in Fig. 5, to form a second- and third-order interpolation for convection (STOIC) scheme. An ad-hoc linear function is used in the [0-0.2] segment of the NVD diagram to enforce the CBC condition f(0) = 0. The functional relationship of the STOIC scheme passes through points (0,0) and (1,1) and satisfy the rest of the CBC conditions. This functional relationship is illustrated in Fig. 5 and is given by

$$\tilde{\phi}_{f} = f(\tilde{\phi}_{C}) = \begin{cases}
\tilde{\phi}_{f} = 3\tilde{\phi}_{C} & \text{for } 0 < \tilde{\phi}_{C} < 0.2 \\
\tilde{\phi}_{f} = \frac{1}{2}(1 + \tilde{\phi}_{C}) & \text{for } 0.2 < \tilde{\phi}_{C} < 0.5 \\
\tilde{\phi}_{f} = \frac{3}{8} + \frac{3}{4}\tilde{\phi}_{C} & \text{for } 0.5 < \tilde{\phi}_{C} < \frac{5}{6} \\
\tilde{\phi}_{f} = 1 & \text{for } \frac{5}{6} < \tilde{\phi}_{C} < 1 \\
\tilde{\phi}_{f} = \tilde{\phi}_{C} & \text{elsewhere}
\end{cases} (13)$$

The functional relationships for the rest of the tested high-resolution schemes are given in Table 2, while their NVD plots are given in Fig. 6. It is seen that the functional relationships in Table 2 are nonlinear; this is generally true of all HR schemes.

Because these HR schemes involve two upstream nodes for each cell face, it is necessary to follow special practices for the near-boundary control volumes. In the present work, the UPWIND scheme is used whenever an upstream node lies outside the computational domain.

APPLICATIONS

In what follows, we present the results of calculations for three test situations that are linear problems involving purely convective transports of scalars containing discontinuities or large gradients. In all tests, the computational results were considered "converged" when the residual error given by Eq. (14) became smaller

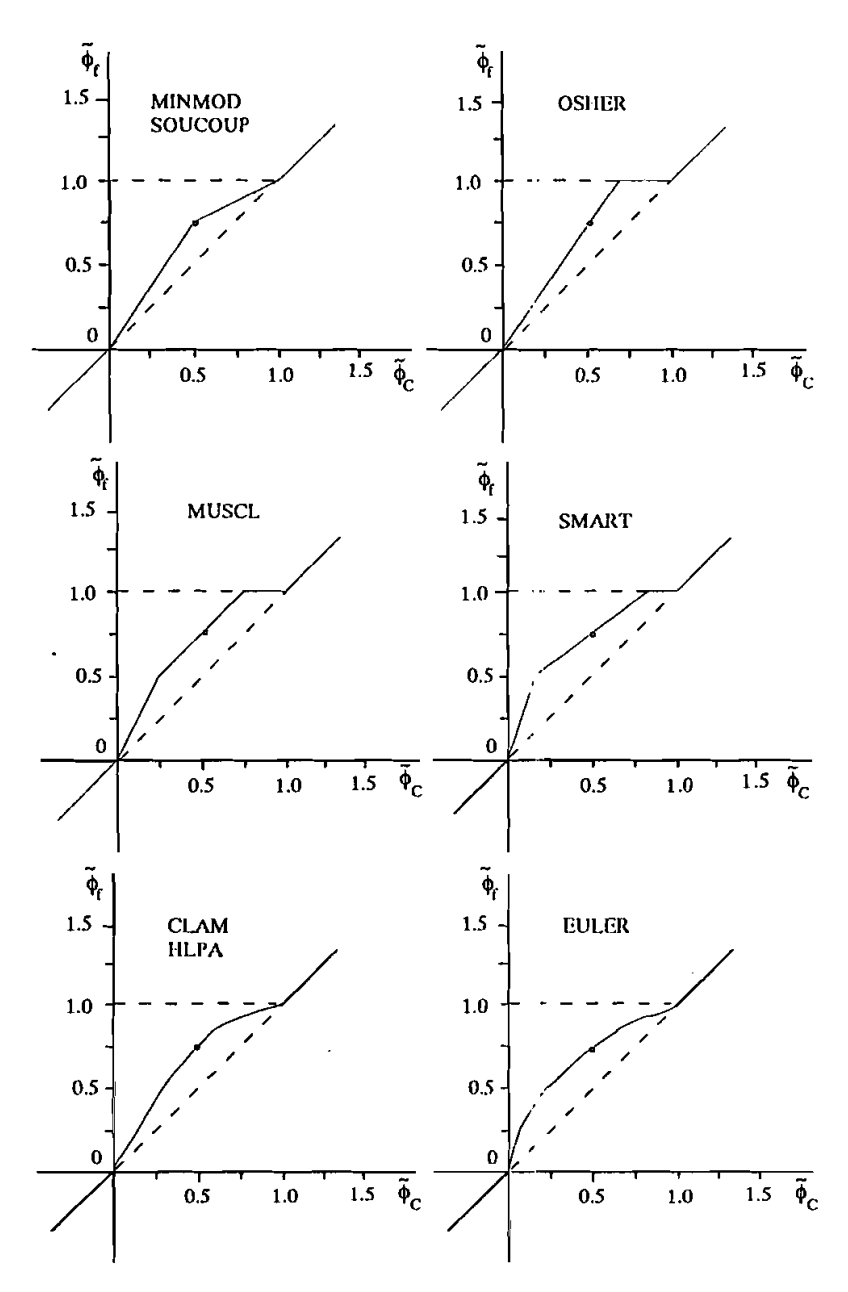


Fig. 6 NVD plots for various high-resolution schemes.

Table 2 Functional Relationships for the Different High-Resolution Schemes

Scheme	Functional relationship $[\tilde{\phi}_f = f(\tilde{\phi}_C)]$		
	Functional relationship $[\phi_f = f(\phi_C)]$ $\begin{cases} \tilde{\phi}_f = \frac{3}{2}\tilde{\phi}_C & \text{for } 0 < \tilde{\phi}_C < \frac{1}{2} \\ \tilde{\phi}_f = \frac{1}{2}(1 - \hat{\phi}_C) & \text{for } \frac{1}{2} < \tilde{\phi}_C < 1 \\ \tilde{\phi}_f = \tilde{\phi}_C & \text{elsewhere} \end{cases}$ $\begin{cases} \tilde{\phi}_f = \frac{3}{2}\tilde{\phi}_C & \text{for } 0 < \tilde{\phi}_C < \frac{2}{3} \\ \tilde{\phi}_f = 1 & \text{for } \frac{2}{3} < \tilde{\phi}_C < 1 \\ \tilde{\phi}_f = \tilde{\phi}_C & \text{elsewhere} \end{cases}$ $\begin{cases} \phi_f = 2\tilde{\phi}_C & \text{for } 0 < \tilde{\phi}_C < \frac{1}{4} \\ \tilde{\phi}_f = 1 & \text{for } \frac{1}{4} < \tilde{\phi}_C < \frac{3}{4} \\ \tilde{\phi}_f = 1 & \text{for } \frac{3}{4} < \tilde{\phi}_C < 1 \\ \tilde{\phi}_f = \tilde{\phi}_C & \text{elsewhere} \end{cases}$ $\begin{cases} \tilde{\phi}_f = \tilde{\phi}_C & \text{elsewhere} \\ \tilde{\phi}_f = \tilde{\phi}_C & \text{elsewhere} \end{cases}$ $\begin{cases} \tilde{\phi}_f = \tilde{\phi}_C & \text{for } 0 < \tilde{\phi}_C < 1 \\ \tilde{\phi}_f = \tilde{\phi}_C & \text{elsewhere} \end{cases}$ $\begin{cases} \tilde{\phi}_f = 3\tilde{\phi}_C & \text{for } 0 < \tilde{\phi}_C < \frac{1}{6} \\ \tilde{\phi}_f = 1 & \text{for } \frac{5}{6} < \tilde{\phi}_C < 1 \\ \tilde{\phi}_f = \tilde{\phi}_C & \text{elsewhere} \end{cases}$ $\begin{cases} \tilde{\phi}_f = \tilde{\phi}_C & \text{for } 0 < \tilde{\phi}_C < \frac{5}{6} \\ \tilde{\phi}_f = 1 & \text{for } \frac{5}{6} < \tilde{\phi}_C < 1 \\ \tilde{\phi}_f = \tilde{\phi}_C & \text{elsewhere} \end{cases}$ $\begin{cases} \tilde{\phi}_f = \tilde{\phi}_C & \text{elsewhere} \end{cases}$		
MINMOD or SOUCOUP	$\begin{cases} \tilde{\phi}_{\rm f} = \frac{1}{2}(1 - \hat{\phi}_{\rm C}) & \text{for } \frac{1}{2} < \tilde{\phi}_{\rm C} < 1 \\ \tilde{\phi}_{\rm C} = \tilde{\phi}_{\rm C} \end{cases}$		
	$\phi_{\rm f} = \phi_{\rm C}$ elsewhere		
	$\int \tilde{\phi}_{\rm f} = \frac{3}{2} \tilde{\phi}_{\rm C} \qquad \text{for } 0 < \tilde{\phi}_{\rm C} < \frac{2}{3}$		
OSHER	$\begin{cases} \tilde{\phi}_{\rm f} = 1 & \text{for } \frac{2}{3} < \tilde{\phi}_{\rm C} < 1 \end{cases}$		
	$\left(ilde{\phi}_{\mathrm{f}} = ilde{\phi}_{\mathrm{C}} ight.$ elsewhere		
	$\phi_{\rm f} = 2\tilde{\phi}_{\rm C} \qquad \qquad \text{for } 0 < \tilde{\phi}_{\rm C} < \frac{1}{4}$		
MUSCL	$\begin{cases} \tilde{\phi}_{\rm f} = \frac{1}{4} + \tilde{\phi}_{\rm C} & \text{for } \frac{1}{4} < \tilde{\phi}_{\rm C} < \frac{3}{4} \end{cases}$		
	$\tilde{\phi}_{\rm f} = 1$ for $\frac{3}{4} < \tilde{\phi}_{\rm C} < 1$		
	$\left(ilde{\phi}_{\mathrm{f}} = ilde{\phi}_{\mathrm{C}} ight.$ elsewhere		
CLAM or HLPA	$\begin{cases} \tilde{\phi}_{\rm f} = \tilde{\phi}_{\rm C}(2 - \tilde{\phi}_{\rm C}) & \text{for } 0 < \tilde{\phi}_{\rm C} < 1 \end{cases}$		
	$\phi_{\rm f} = \phi_{\rm C}$ elsewhere		
	$\tilde{\phi}_{\rm f} = 3\tilde{\phi}_{\rm C}$ for $0 < \tilde{\phi}_{\rm C} < \frac{1}{6}$		
SMART	$\begin{cases} \tilde{\phi}_{\rm f} = \frac{3}{8} + \frac{3}{4}\tilde{\phi}_{\rm C} & \text{for } \frac{1}{6} < \tilde{\phi}_{\rm C} < \frac{5}{6} \end{cases}$		
	$\tilde{\phi}_{\rm f} = 1$ for $\frac{5}{6} < \tilde{\phi}_{\rm C} < 1$		
	$ ilde{\phi}_{f} = ilde{\phi}_{C}$ elsewhere		
EULER	$\begin{cases} \tilde{\phi}_{\rm f} = \tilde{\phi}_{\rm C} & \text{elsewhere} \\ \begin{cases} \frac{2}{\sqrt{\tilde{\phi}_{\rm C}(1 - \tilde{\phi}_{\rm C})^3} - \tilde{\phi}_{\rm C}^2} \\ (1 - 2\tilde{\phi}_{\rm C}) \end{cases} & \text{for } 0 < \tilde{\phi}_{\rm C} < 1 \\ 0.75 & \text{for } \tilde{\phi}_{\rm C} = 0.5 \\ \tilde{\phi}_{\rm C} & \text{elsewhere} \end{cases}$		
	$0.75 for ilde{\phi}_{\rm C} = 0.5$		
_	$\hat{\phi}_{ ext{C}}$ elsewhere		

than 0.08%,

$$RES = \sum \left| a_{p} \phi_{P} - \left(\sum_{nb} a_{nb} \phi_{nb} - b_{P} + b_{dc} \right) \right|$$
 (14)

and the quantitative indication of the error was calculated from Eq. (15),

$$\epsilon = \sum |\phi_{\text{computed}} - \phi_{\text{exact}}| \tag{15}$$

summed over all computed grid points.

Convection of a Step Profile in an Oblique Velocity Field

Figure 7 shows the well-known benchmark test problem consisting of a pure convection of a transverse step profile imposed at the inflow boundaries of a square computational domain; a 25×25 mesh was used, giving in this case $\Delta x = \Delta y = \frac{1}{25}$. The location of the boundary step was chosen so that the exact convected step passes through the midpoint of the grid. The angle θ was chosen to be 30.92° and |V| = 1, so as to have the analytical profile coincide with grid nodes in the last grid column.

A comparison of the numerical solution obtained with the different HR schemes and the upwind scheme is shown in Figs. 8 and 9 along with the exact solution. It can be seen very clearly that the upwind scheme results in a very diffuse ϕ profile, while the HR schemes except for MINMOD scheme result in an adequate ϕ profile. However, looking at Table 3, we can assess the performance of the different schemes more accurately. It is clear that the STOIC scheme gives the least error, followed by the SMART, MUSCL, and EULER schemes. The MINMOD is relatively very diffusive, resulting in an error twice that of the STOIC scheme.

Convection of an Elliptic Profile in an Oblique Velocity Field

An elliptic profile was also used for the same geometric situation. This second problem, also illustrated in Fig. 7, was used in order to test the resolution of

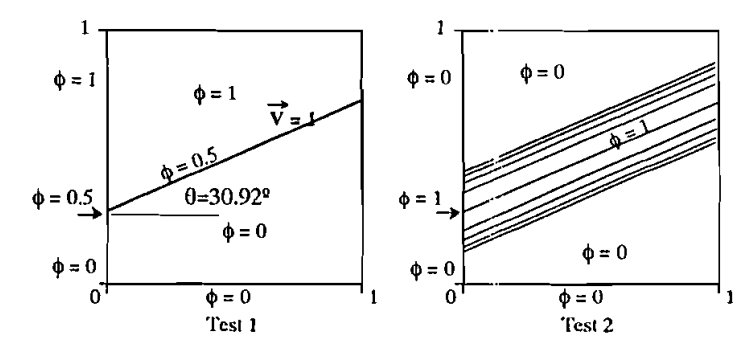
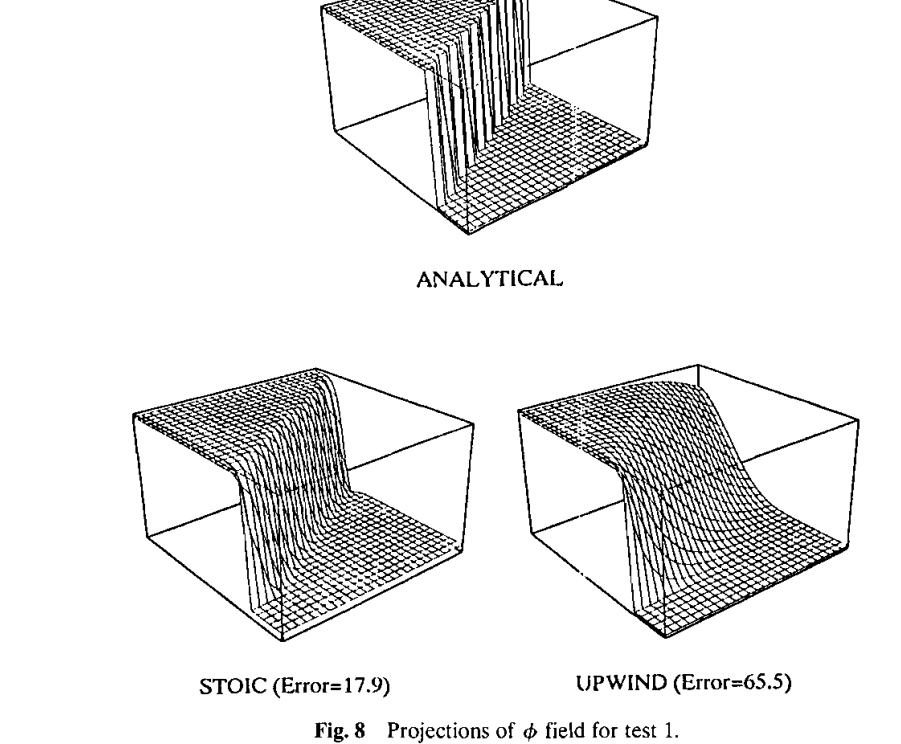


Fig. 7 Pure convection of a scalar discontinuity and an elliptic profile by a uniform velocity field.



the different schemes for a profile involving a gradually decreasing gradient. The elliptic profile is generated using the following equation:

$$\phi = \sqrt[2]{1 - \frac{\left[j + \left(\frac{1}{5}\right)\right]^2}{\left(\frac{9}{25}\right)^2}} \quad \text{for } 2 \le j \le 12$$
 (16)

The same mesh was used as for test 1.

As before, the computational results for the HR schemes, the UPWIND scheme, and the exact solution are shown in Figs. 10 and 11. The ϕ profiles of the UPWIND and MINMOD schemes are clearly very diffuse. It is worth noting that, as indicated in Table 3, the range of error is greater than that for test 1, the UPWIND scheme giving an error of 93.3 as compared to 65.5. However, the STOIC still presents the least error. This can also be noticed in Fig. 10 by the close resemblance of its ϕ profile with the exact solution profile; however, a slight flattening of the profile can also be observed.

Smith-Hutton Problem

In the third test problem, shown in Fig. 12, a step discontinuity at x = -0.5 is convected clockwise from the inlet plane (x < 0, y = 0) to the outlet plane

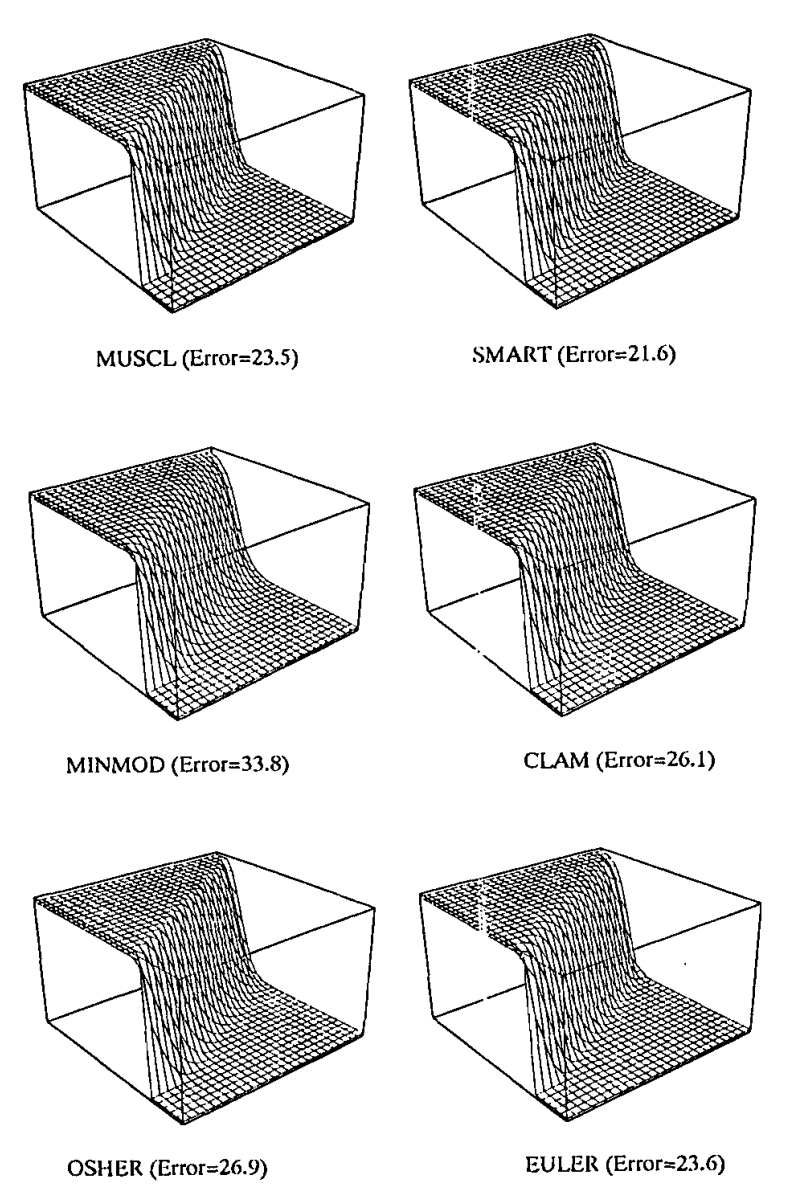


Fig. 9 Projections of ϕ field for test 1.

(x > 0, y = 0) by a rotational velocity field given by

$$u = 2y(1 - x^{2})$$

$$v = -2x(1 - y^{2})$$
(17)

This test was devised for evaluating a number of numerical models of convection at the third meeting of the International Association for Hydraulic Research Working

Scheme ERROR (test 1) ERROR (test 2) ERROR (test 3) **UPWIND** 65.5 93.3 41.3 MINMOD 33.8 40.6 24.7 (SOUCOUP) **OSHER** 26.9 30.2 20.0 CLAM (HLPA) 26.1 27.5 20.3 **EULER** 23.6 22.5 22.5

Table 3 ERROR for the Different Schemes and the Different Tests

23.5

21.6

17.9

MUSCL

SMART

STOIC

Group on Refined Modelling of Flow [1], but in this problem we have

$$\phi = \begin{cases} 0 \text{ for } -0.5 < x < 0 & y = 0\\ 2 \text{ for } -1 < x < -0.5 & y = 0\\ 2 \text{ for } -1 < x < 1 & y = 1\\ 2 \text{ for } x = -1 & 0 < y < 1\\ 2 \text{ for } x = 1 & 0 < y < 1 \end{cases}$$
(18)

23.3

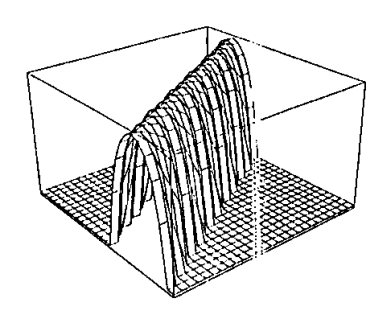
20.0

16.2

18.4

17.0

15.1



ANALYTICAL

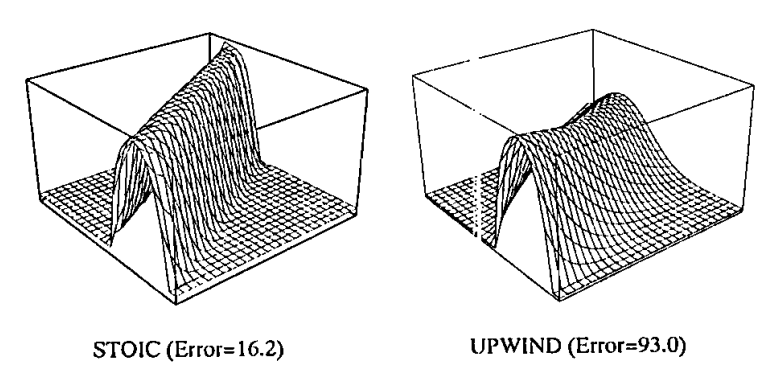


Fig. 10 Projections of ϕ field for test 2.

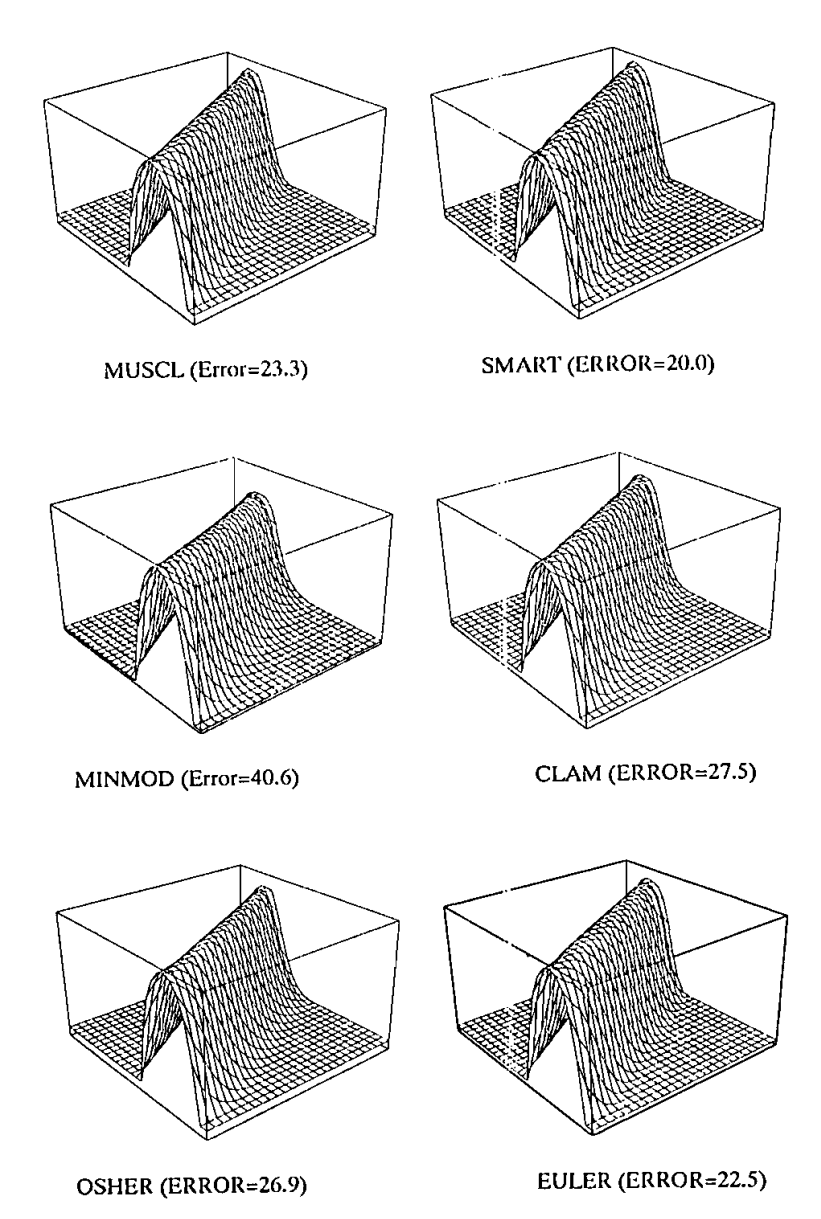


Fig. 11 Projections of ϕ field for test 2.

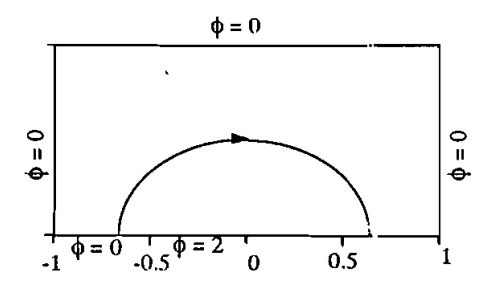


Fig. 12 Test 3, pure convection by a rotational velocity field.

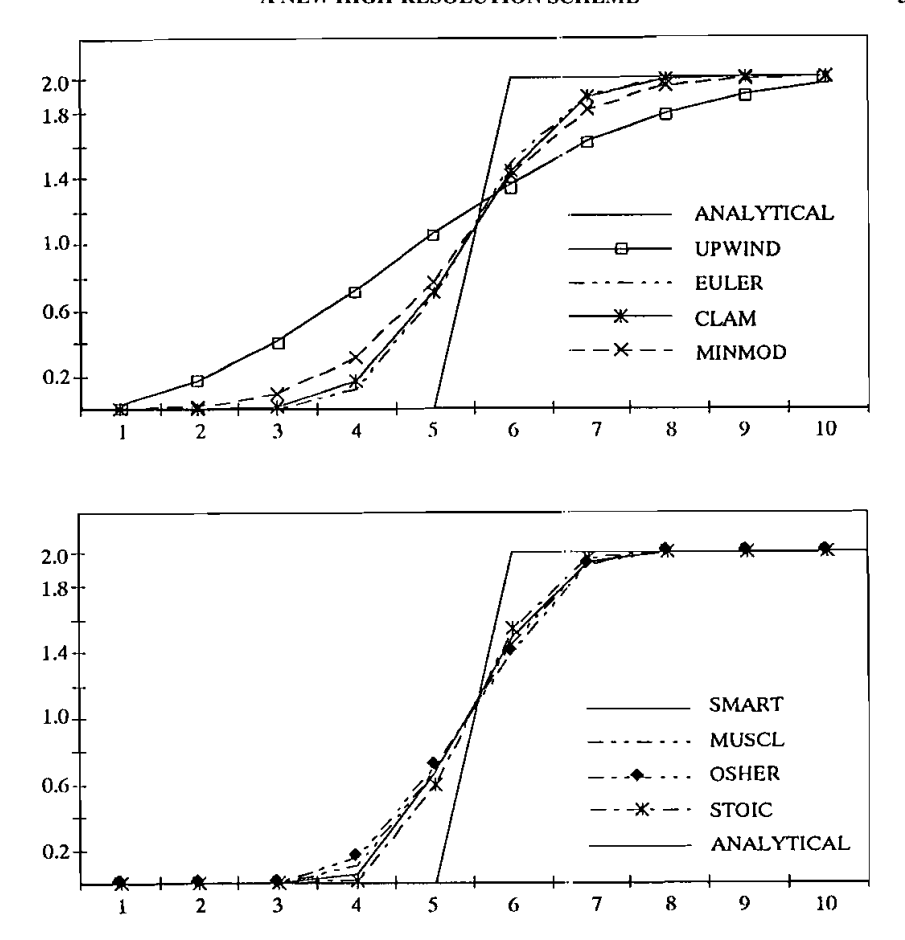


Fig. 13 Comparison of ϕ profiles at exit for test 3.

In this test no physical diffusion was set, and a 20×10 mesh was used, yielding $\Delta x = \Delta y = \frac{1}{10}$. The results for this test are shown in Fig. 13. The STOIC scheme still gives the most accurate profile as in the previous tests.

In all three tests, the computational time for the HR schemes on the average of the order of four to five times the computation time of the UPWIND schemes, with schemes involving more than one breakpoint, such as the SMART and STOIC, being the most expensive in computational time. All the HR schemes do not exhibit any undue over/undershoot, in all tests the MINMOD is shown to be the most diffusive as can be expected from its NVD plot, while the STOIC and SMART give the most accurate results, the STOIC being slightly more accurate. Table 3 shows the errors for all the test problems quantitatively.

The increase of accuracy of the STOIC scheme over the SMART scheme is due to the more compressive linear function used in the interval [0.2, 0.5] of the NVD plot. Other, more compressive schemes can be devised, such as Roe's SuperBee scheme [27], but it would be expected that these schemes will yield less accurate results than the STOIC (or SMART) scheme, due to substantial false compression, that is, the tendency to flatten round profiles.

CONCLUSION

In this article, a number of schemes formulated using the NVF methodology have been tested. Furthermore, a composite convection scheme, based on the normalized variable formulation (NVF) of Leonard, has been proposed for finite-volume calculations of incompressible steady flows. The scheme, involving a second- and third-order interpolation profile in the monotonic region, is relatively simple to implement and is stable, bounded, and highly accurate. The scheme was tested for three situations involving large gradients, and in all three tests the accuracy of the computed results by the present method was found to be superior to that of the CLAM, MUSCL, EULER, MINMOD, and OSHER schemes, and better than the SMART scheme. All these desired features, combined with ease of implementation due to the deferred correction procedure, make the present scheme a good alternative to many existing schemes, specifically to the first-order upwind scheme that is unfortunately still widely used in the CFD community.

REFERENCES

- 1. R. M. Smith and A. G. Hutton, The Numerical Treatment of Advection: A Performance Comparison of Current Methods, *Numer. Heat Transfer*, vol. 5, pp. 439–461, 1982.
- 2. B. P. Leonard, A Stable and Accurate Convection Modelling Procedure Based on Quadratic Interpolation, *Comp. Meth. Appl. Mech. Eng.*, vol. 19, pp. 59–98, 1979.
- 3. R. K. Agarwal, A Third Order Accurate Upwind Scheme for Navier Stokes Solutions in Three Dimensions, in K. N. Ghia, T. J. Mueller, and B. R. Patel (eds.), *Computers in Flow Prediction and Fluid Dynamics Experiments. ASME Winter Meeting*, Washington, D.C., pp. 73–82, 1981.
- 4. E. A. Fromm, A Method for Reducing Dispersion in Convective Difference Schemes, J. Comput. Phys. vol. 3, pp. 176-189, 1968.
- S. A. Syed, L. M. Chiappetta, and A. D. Gosman, Error Reduction Program: Final Report NASA Contractor Report NASA-CR-174776, 1985.
- A. Turan and J. P. Van Doormaal, Improved Numerical Methods for Turbulent Viscous Recirculating Flows, NASA Contractor Report NASA-CR-180852, 1988.
- 7. S. T. Zalesak, Fully Multidimensional Flux-Corrected Transport Algorithms for Fluids, J. Comput. Phys., vol. 31, pp. 335-362, 1979.
- 8. M. Chapman, FRAM Nonlinear Damping Algorithm for the Continuity Equation, J. Comput. Phys., vol. 44, pp. 84-103, 1981.
- 9. M. Peric, A Finite Volume Method for the Prediction of Three Dimensional Fluid Flow in Complex Ducts, Ph.D. thesis, Imperial College, London, U.K., 1985.
- J. Zhu and M. A. Leschziner, A Local Oscillation-Damping Algorithm for Higher Order Convection Schemes, Comp. Meth. Appl. Mech. Eng., vol. 67, pp. 355–366, 1988.
- 11. D. B. Spalding, A Novel Finite-Difference Formulation for Differential Expressions Involving Both First and Second Derivatives, *Int. J. Numer. Meth. Eng.*, vol. 4, pp. 551-559, 1972.
- 12. S. V. Patankar, Numerical Heat Transfer and Fluid Flow, Hemisphere, Washington, D.C., 1981.
- 13. P. K. Sweby, High Resolution Schemes Using Flux Limiters for Hyperbolic Conservation Laws, SIAM J. Numer. Anal., vol. 21, pp. 995-1011, 1984.
- 14. B. P. Leonard, Simple High-Accuracy Resolution Program for Convective Modelling of Discontinuities, *Int. J. Numer. Meth. Eng.*, vol. 8, pp. 1291–1318, 1988.
- 15. B. P. Leonard, A Survey of Finite Differences with Upwinding for Numerical Modelling

- of the Incompressible Convection Diffusion Equation, in C. Taylor and K. Morgan, (eds.), Computational Techniques in Transient and Turbulent Flow, Pineridge Press, Swansea, U.K., vol. 2, pp. 1–35, 1981.
- 16. J. Zhu and W. Rodi, A Low Dispersion and Bounded Convection Scheme, *Comp. Meth. Appl. Mech. Eng.*, vol. 92, pp. 87-96, 1991.
- 17. P. H. Gaskell and A. K. C. Lau, Curvature Compensated Convective Transport: SMART, a New Boundedness Preserving Transport Algorithm, *Int. J. Numer. Meth. Fluids*, vol. 8, pp. 617–641, 1988.
- 18. J. Zhu, A Low-Diffusive and Oscillation-Free Convection Scheme, *Commun. Appl. Numer. Meth.*, vol. 7, pp. 225–232, 1991.
- H. Lin and C. C. Chieng, Characteristic-Based Flux Limiters of an Essentially Third-Order Flux-Splitting Method for Hyperbolic Conservation Laws, *Int. J. Numer. Meth. Fluids*, vol. 13, pp. 287-307, 1991.
- 20. B. Van Leer, Towards the Ultimate Conservative Difference Scheme. V. A Second-Order Sequel to Godunov's Method, *J. Comput. Phys.*, vol. 23, pp. 101-136, 1977.
- 21. B. Van Leer, Towards the Ultimate Conservative Difference Scheme. II. Monotonicity and Conservation Combined in a Second Order Scheme, *J. Comput. Phys.*, vol. 14, pp. 361–370, 1974.
- 22. S. R. Chakravarthy and S. Osher, High Resolution Application of the OSHER Upwind Scheme for the Euler Equations, AIAA Paper 83–1943, 1983.
- 23. A. Harten, High Resolution Schemes for Hyperbolic Conservation Laws, *J. Comput. Phys.*, vol. 49, no. 3, pp. 357-393, 1983.
- B. P. Leonard, The EULER-QUICK Code, in C. Taylor and K. Morgan (eds.), Numerical Methods in Laminar and Turbulent Flows, Pineridge Press, Swansea, U.K., 1983.
- 25. B. P. Leonard, The ULTIMATE Conservative Difference Scheme Applied to Unsteady One-Dimensional Advection, *Comp. Meth. Appl. Mech. Eng.*, vol. 88, pp. 17–74, 1991.
- S. G. Rubin and P. K. Khosla, Polynomial Interpolation Method for Viscous Flow Calculations, J. Comput. Phys., vol. 27, pp. 153-168, 1982.
- 27. P. L. Roe, in E. Enquist, S. Osher, and R. J. C. Sommerville (eds.), *Large Scale Computations in Fluid Mechanics*, *Part 2* (Lectures in Applied Mathematics, Vol. 22) Springer Verlag, pp. 163-193, 1985.

Received 29 October 1992 Accepted 11 May 1993

Address correspondence to M. S. Darwish, American University of Beirut, Faculty of Engineering & Architecture, Mechanical Engineering Department, 850 Third Avenue, 18th Floor, New York, NY 10022, USA.